Density-functional calculation for K lattices in condensed phase and quantum-chemical model for the cohesive energy of heavy alkali metals

N. H. March and Angel Rubio
Departamento de Física Teórica, Universidad de Valladolid, E-47011 Valladolid, Spain
(Received 4 December 1996; revised manuscript received 11 July 1997)

Following a summary of deductions from experiment on the bonding of Rb and Cs in very different liquid and solid environments, energy calculations based on density-functional theory (DFT) are presented on ordered chains of K as a function of nearest-neighbor distances. At a given bond length, and sufficiently low density, a regime occurs in which modest zig-zag behavior is found to stabilize the original linear chains. As for Rb and Cs, we conclude that K may exhibit low coordination in highly expanded forms. The previous *ab initio* results on lattices of K atoms for coordination numbers $z=8$, 4, and 2 are analyzed by means of a quantum-chemical model in which a nearest-neighbor Heisenberg Hamiltonian is characterized by free-space K_2 dimer potential energy curves. The satisfactory accord between the two different treatments has prompted us to present results also for Rb and Cs lattices for five different coordination numbers for which DFT calculations are not currently available. The relevance to experiments on expanded fluid Cs and to zig-zag chains of Cs on semiconductor substrates is briefly referred to. [S0163-1829(97)02445-4]

I. INTRODUCTION

In pioneering work on the measurement of liquid structure factors $S(q)$ using neutron diffraction, Hensel *et al.*[1,2] have studied liquid metallic Rb and Cs in a number of thermodynamic states along the liquid-vapor coexistence curve towards the critical point. Their findings were that the high coordination numbers just above freezing, compatible with the local coordination in the hot bcc solids, were progressively lowered as these heavy alkali liquid metals were highly expanded. At the same time, it was found that the nearest-neighbor distance remained largely intact, as evidenced by the position of the main peak in $S(q)$ remaining at almost constant value of $q_{\max}$. These findings suggested the study of different phases (with different coordination numbers) for expanded alkali metals for a fixed nearest-neighbor distance (see below).

One of us[3] noted that the coordination number data of Hensel *et al.*,[1,2] when plotted against mass density d, could be fitted by

$$d = az + b, \tag{1}$$

where $a=230$ and $b=-80$, both in kg/m^3. For a low-density state of Cs described by Winter and Hensel,[2] with atomic number density $\rho=0.004\,16$ Å^{-3} and temperature $T=1923$ K, pair potentials $\phi(r)$ were extracted from the measured $S(q)$ by Ascough and March,[4] following the proposal of Johnson and March.[5] One of these potentials[4] (dashed curve) is compared with a theoretical pair potential obtained by Arai and Yokoyama[6] in Fig. 1 (continuous line). This potential has a sharp minimum at 5.6 Å followed by a repulsive region out to ~ 9 Å (with the maximun at $\sim$8.5 Å) and a second minima at $\sim$9.4 Å. We shall return to consequences of these pair interactions for expanded liquid metal Cs below.

Turning from these liquid metals, with short-range order (SRO) characterized by $S(q)$, we next consider a quite different type of study made by Whitman *et al.*[7,8] In their work, Cs was deposited on semiconductor crystal surfaces, and as a result data has, subsequent to the experiments of Hensel *et al.* on SRO, become available on expanded Cs structures with long-range order (LRO). While, as emphasized by Freeman and March,[9] this data is at least partially about Cs in interaction with the semiconducting substrate, there is nevertheless again an important message about chemical bonding in highly expanded Cs, but this time with LRO. Specifically, Whitman *et al.*[7] have measured the structural properties of Cs adsorbed on GaAs(110) and InSb(110) surfaces at room temperature using scanning tunneling microscopy. Their work establishes that Cs initially forms long, one-dimensional zig-zag chains on both these surfaces. To take one example,[7,9] their Fig. 1(a) shows a large-area image of Cs chains on GaAs(110) that includes chains more than 1000 Å in length. Their experiments conclusively demonstrate, in addition, that the chains tend to be separated by some tens of nm and have no LRO along the [001] direction; thus establishing that they are truly one-dimensional structures.[7] In their Fig. 1(b), showing the higher-resolution image, the Cs structures are revealed as zig-zag chains of single atoms in registry with the substrate (110) surface. In the present context, it is important to stress that the Cs-Cs nearest-neighbor distance here is 6.9 Å, to be compared with the corresponding distance of 5.2 Å in bulk Cs. On the InSb(110) surface, the formation of Cs zig-zag chains was again revealed by the experiments of Whitman *et al.*,[7] but because of InSb having the greatest spacing of the III-V semiconductors, the Cs nearest-neighbor distance is now 8.0 Å. Thus we have a lowering of the coordination of Cs induced by the semiconductor substrate. This is to be compared with the previously discussed lowering of the coordination in an expanded Cs liquid taken along the liquid-vapor coexistence curve toward the critical point. In this last case, it seems to be established beyond reasonable doubt that the building block of the expanded liquid metals Cs and Rb is a chemical bond with a rather constant length of $\sim$5.4–5.7 Å with coordination number between 2 and 3.

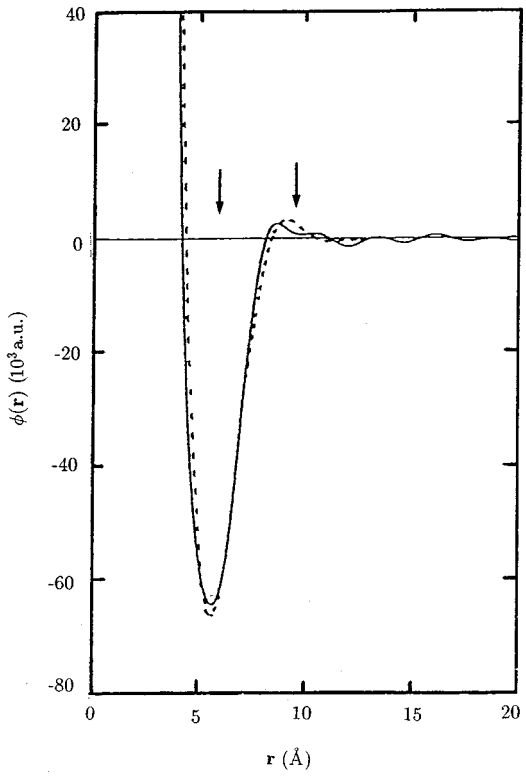

FIG. 1. Pair potentials (in a.u.) for expanded liquid Cs metal from Ref. 6 (continuous line) and Ref. 4 (dashed line) corresponding to an atomic density $\rho = 0.004\,16$ Å^{-3} and temperature $T = 1923$ K. The vertical arrows indicate the position of the nearest and next-nearest neighbor for the hypothetical diamond structure of expanded Cs. The comparison with the theoretical pair potential given by the continuous line shows qualitatively that the potential at this density and temperature tends to favor low coordination structures.

These key experiments[1,2,7] have therefore led us to study further, by density-functional theory (DFT), the energetics of chains of alkali atoms. For calculational purposes, we have chosen to focus on K, rather than Rb and Cs investigated in the experiments on condensed conducting phases summarized above because their pseudopotential generation is less certain due to relativistic and *d*-electron effects (see below). The paper is organized as follows: first we briefly describe the theoretical model used and the results obtained for high- and low-coordinated K lattices. Then we use this data in conjunction with available pair potentials at different thermodynamic states to discuss the local coordination of the low-density heavier alkalis in condensed phases. We shall later bring these DFT results for K into contact with a simple and physically appealing quantum-chemical model proposed by March, Tosi, and Klein.[10] Then, encouraged by the agreement of this model with the DFT data, we extend the results from the quantum-chemical model to Rb and Cs for which DFT calculations are not available. Some conclusions are given at the end of the paper.

II. THEORETICAL METHOD

We have performed the *ab initio* band-theory calculations within the framework of density-functional theory. Briefly, we employ the standard plane-wave pseudopotential total-energy scheme[11,12] in the local-density approximation (LDA) (Ref. 13) to the exchange correlation potential $V_{xc}(\mathbf{r})$ to describe the ground state. *Ab initio* norm-conserving nonlocal ionic pseudopotentials have been generated by the soft-pseudopotential method of Troulliers and Martins[14] including nonlinear core corrections.[15] These core corrections are important to describe the structural properties of systems with shallow core levels close to the valence complex,[15] as it is the case here. The LDA wave functions were expanded up to a 10-Ry cutoff where good convergence in total energy was achieved (see Refs. 11 and 12 for details of the method). The other essential input, besides of course the nearest-neighbor distance and the angle (or height) of the zig-zag chains considered, was the exchange-correlation potential $V_{xc}(\boldsymbol{r})$ in constructing the total periodic potential $V(\boldsymbol{r}) = V_{\text{Hartree}}(\boldsymbol{r}) + V_{xc}(\boldsymbol{r})$. $V_{\text{Hartree}}(\boldsymbol{r})$ is, of course, determined by the geometry of the lattice plus the ground-state electron density $n(\boldsymbol{r})$ and in the local-density approximation used to construct $V_{xc}(\boldsymbol{r})$. This is again specified by $n(\boldsymbol{r})$ alone.

The calculations for open structures as the linear and zig-zag chains were performed in a supercell geometry scheme. We keep the real periodicity of the structure along the chain direction and introduce a large vacuum region in the other two directions in order to minimize the chain-chain interaction (using a distance between chains of 9 Å). The set of three-dimensional structures (crystalline phases) were computed for different fixed symmetries and nearest-neighbor distances.

TABLE I. Equilibrium structural properties for different phases of K as shown in Fig. 2. The zig-zag chain data are not reported because they depend strongly on zig-zag angle or coordination, see Fig. 2. The pseudoatom energy used as a reference is 7.95 eV. The shorter bond length [nearest-neighbor NN distance] corresponds to the dimer (3.90 Å) and this increases when the coordination increases (the diamond structure has the shortest bond length due to the larger structural packing). In parentheses in the Table are given the experimental values for the bcc-K bulk phase.

	NN distance (Å)	E_{coh} (eV/atom)	Bulk modulus (GPa)
K-bcc	4.42 (4.52)	1.08 (0.94)	4.0 (3.3)
K-diamond	4.02	0.80	1.41
Linear chain	4.00	0.32	

III. LOCAL COORDINATION OF LOW-DENSITY ALKALIS IN CONDENSED PHASES

Table I records the results of these *ab initio* calculations for the normal bcc-K phase and other hypothetical phases such as the diamond and the metallic-linear chain (not Peierls distorted, see below) that are not realizable in normal conditions (coordinations ranging from 2 to 8). The agreement for the bcc-K phase with experimental data is good (within the typical LDA few-percent errors for lattice constant, bulk modulus, and cohesive energy). As expected, the computed equilibrium $T = 0$ nearest-neighbor distance increases with increasing coordination (as well as the cohesive energy). Thus external forces such as substrate induced registration, temperature, or pressure would determine the type

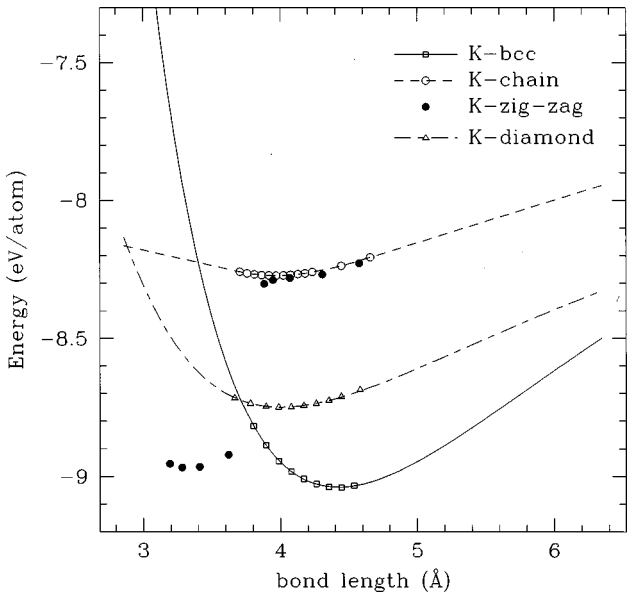

FIG. 2. Total energy per atom for different K phases as a function of the nearest-neighbor distance. For bond-lengths larger than 4.50 Å, the zig-zag and linear chains coincide. The set of values for zig-zag chains with bond lengths lower than 4 Å corresponds to the formation of nearly equilateral triangles (coordination ~ 4 instead of 2 for the linear or small deformed zig-zag chains) including some chain-chain interactions. We note that for a given bond length of the zig-zag chain the structure is minimized with respect to the zig-zag angle. This angle tends to be 180° (linear chain) with increasing bond length, from the ''delocalized molecular orbitals'' treatment used to construct this figure.

of coordination shown by these alkali metals.[16] We note that the nearest-neighbor distance for the linear chain is close to the experimental dimer bond length of 3.90 Å.[17] For what follows we are interested in the low-density (expanded bond length) region where low-coordination phases are more likely to be obtained (see also Fig. 2). We think of the expanded metal as formed by a set of tangled zig-zag chains with coordination between 2 to 4 depending of the nearest-neighbor distance. In this low-density regime we have found a very small chain-chain interaction, however when density increases it becomes important and favors the formation of three-dimensional structures. As a remark, the results presented in Fig. 2 are obtained at $T=0$ for the crystalline phases, and therefore the three-dimensional structures are lower in energy than the low-coordinated phases; however these LRO models are only illustrative to mimic the SRO in the liquid metals.

The energetics of a linear chain of equidistant K atoms is compared from the DFT calculations with the energy per atom of a planar zig-zag chain in Fig. 2. For a sufficiently large nearest-neighbor distance, it is found that a modest zig-zag, for fixed nearest-neighbor distance, lowers the energy and hence results in a stabilization of the phase.[18] For longer distances there is no stable zig-zag chain. We must stress, however, that in the long nearest-neighbor distance regime the band-structure calculations the way they are performed here should be viewed with some caution because correlations beyond those included through the LDA exchange-correlation potential might become very important in this regime (see below). Thus, for expanded K metal either modest zig-zag chains or linear chains could be formed.

TABLE II. Position in Å of the prominent features in the DFT theory pair potential of liquid K near freezing ($T=65$°C). [M. W. Johnson, N. H. March, F. Perrot, and A. K. Ray, Philos. Mag. B **69**, 965 (1994)]. When the nearest-neighbor distance is fixed to the principal minimum value the next-nearest-neighbor distance for the bcc structure is 5.42 Å (well within the first potential well), whereas for the lower coordination diamond it is 7.6 Å (very close to the repulsive maximum). This indicates qualitatively that the potential near freezing tends to favor high coordination structures (see text).

Average density	First node	Principal minimum	First maximum	Second node
0.001 882 6	4.02	4.69	7.33	6.56

This is a convenient point at which to return to the interionic potentials in Fig. 1. From Eq. (1), this thermodynamic state corresponds to a coordination number between 2 and 3. In principle, neglecting the density change on freezing, we could use the theoretical pair potential given by continuous line in Fig. 1 to compare energies of different crystal structures at constant volume (i.e., not now at constant nearest-neighbor distance). What we have done instead is to mark on Fig. 1, for a nearest-neighbor distance put equal to that in expanded metallic bcc Cs (5.63 Å), where the next-nearest-neighbor distances, etc., would lie for the diamond structure with coordination number 4. The next-nearest-neighbor distance for the diamond structure is 9.2 Å, to be compared with the 9.7 Å of a 3-fold coordination structure such as graphite (note that the pair potential reaches its maximum repulsive part at ~ 9 Å followed by a flat second minimum where the next nearest-neighbor distances of the low-coordinated structures lie). This qualitative argument indicates that low local coordination is favored for the expanded condensed phase of Cs in agreement with the experimental observation from Eq. (1). In order to get more insight for a different thermodynamic limit, we have also given in Table II the data for a DFT pair potential of liquid K near freezing the position of minimum and maximum of the potential. When fixing the first-nearest-neighbor distance to the position of the principal minimum (4.69 Å) we get a next-nearest neighbor distance of 5.4 and 7.6 Å for the bcc and diamond structures, respectively. In contrast to what happens in Fig. 1, where the lower coordination structure seems to be favored by the potential, near freezing the diamond peak lies just close to the maximum of the potential (located only $\sim 3.5\%$ beyond the maximum of the potential for liquid K given in Table II, while for expanded Cs the peak lies $\sim 9\%$ beyond the maximum and close to the second potential minimum of Fig. 1) and therefore this structure would not be stable when compared to higher coordination structures

Our concluding remarks for this section will focus on the electrical characteristics of the Rb and Cs assemblies in both fluid SRO and ordered LRO phases. Taking the LRO case first, Whitman *et al.*[7] probed for metallic behavior by measuring the tunneling conductivity (reduction of the band gap) at zero bias, which is known to be proportional to the density of states at the Fermi level. Their measured current vs voltage curves showed that the band gap of 1.45 eV of GaAs was lessened to 1.1 eV with the one-dimensional chains of Cs on

the surface, which implies that the Cs chain structures are insulating[7] on GaAs(110) Earlier, one of us[3] had suggested the same conclusion from a chain model for the SRO in fluid Cs but now at the critical density. But there the Peierls transition was invoked to propose the identity of the metal-insulator transition and the critical point in fluid Cs. Whitman *et al.*[7] refer, on the other hand, in support of their experimental approach, to the theoretical study of Ferraz and co-workers[19] in relation to the proximity of bulk Cs to the metal-insulator transition. It may well be asked whether, in the theoretical studies of chains of K reported here, we are also in the vicinity of a metal-insulator transition. We must therefore add that the energy band-theory approach used here, in the context of density-functional theory, bases all its findings on ''delocalized molecular orbitals'' describing the one valence electron per K atom. Even though, of course, some account of electron correlation is incorporated through the exchange-correlation potential, one has, in essence, underlying the treatment, a one-electron Slater-Kohn-Sham single determinant reference wave function. To study the metal-insulator transition, one should follow the Gutzwiller procedure,[20] which is the analogue for crystals of the Coulson-Fischer[21] quantum-chemical treatment of the H_2 molecule. In essence, both these approaches expand out the determinantal wave function and then, by introduction of a variational ''parameter'' $\lambda(r_0)$, one reduces drastically, near the metal-insulator transition, the weights of ''ionic'' configurations in which two electrons are permitted to reside on the same atomic site.[22] Of course, this approach is quite different from the Peierls transition referred to above, in which alternating bond lengths introduce a new energy gap and hence preclude a one-dimensional metal. The LRO experiments above the ''dimerization'' are precluded by substrate Cs interaction and therefore we have not considered such Peierls instability in the LRO calculations on K chains reported here.

IV. QUANTUM-CHEMICAL MODEL FOR THE COHESIVE ENERGY OF ALKALIS

In the previous section we have been concerned with the electronic structure of different lattices of K atoms using density-functional theory with a local-density approximation for the exchange and correlation potential. In particular, the cohesive energy $E_c(z,r_0)$ was calculated as a function of nearest-neighbor distance r_0 for different values of the coordination number z. The values of z explored were $z=8$, corresponding to bulk body-centered-cubic K metal, with equilibrium nearest-neighbor distance $r_0 \sim 4.5$ Å, $z=4$ corresponding to a diamond structure and chains both linear and (modest) zig-zag puckered chains ($z=2$). The purpose of the present section is to focus on a quantum-chemical characterization of the cohesive energy curves of the above lattices.

The idea underlying the analysis to be presented here is to decompose the cohesive energy $E_c(z,r_0)$ into a linear combination of two terms. The first, prmportional to the coordination number z, is to be thought of as a typical pairwise additive contribution, which we shall write in the convenient form $\frac{1}{2}zR(r_0)$, following the notation of March and co-workers.[10] The quantum-chemical interpretation of $R(r_0)$ will be discussed further below. The second term will be written, with appropriate sign as $f(z)g(r_0)$, (Refs. 10 and 23) to yield the approximate form

$$E_c(z,r_0)=\tfrac{1}{2}zR(r_0)-f(z)g(r_0). \tag{2}$$

The second term in Eq. (2), which ''factorizes'' into a function of z, $f(z)$ times $g(r_0)$, in analogy with the first term, is characteristic of the so-called ''glue'' models of solid-state physics, as discussed, for instance, in the early work of Finnis and Sinclair[24] that deals with metallic cohesion as arising from embedding ions in a free-electron gas. For this embedded atom potential the pairwise potential [related to $R(r_0)$] and many-body embedding function [related to $g(r_0)$] are usually fitted to reproduce the equilibrium atomic volume, elastic moduli, and ground-state structure of the perfect lattice. Here, we shall press the relationship of the functions $R(r_0)$ and $g(r_0)$ to properties of the K free space dimer and from this deduce the cohesive energy curves for extended structures. But, for the moment, let us use the form of Eq. (2) to motivate a different plot of the data of Fig. 2. Thus, if the ''linear superposition of factorizable contributions'' in Eq. (2) is useful, we can remove the function $R(r_0)$ by taking the weighted difference of the cohesive energy curves of Fig. 2, namely, $E_c(z=8)-2E_c(z=4)$, $E_c(z=4)-2E_c(z=2)$, and $E_c(z=8)-4E_c(z=2)$. We have therefore plotted these three quantities in Fig. 3.

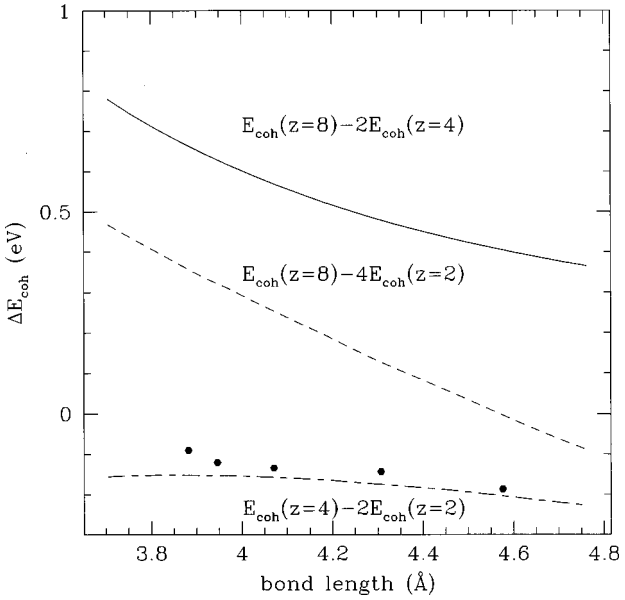

FIG. 3. Weighted cohesive energy difference curves for bcc ($z=8$), diamond ($z=4$), and chain ($z=2$) assemblies of K atoms from the *ab initio* data from Fig. 2 as a function of the nearest-neighbor bond length. Plot motivated by quantum-chemical model in Eq. (2). Using the ''exchange'' function $g(r_0)$ taken from theoretical studies in Ref. 27, we extract the values of $f(z)$ for $z=4$ and 2 as $f(4)=2.9$ and $f(2)=1.3$ (see text).

The upper two curves of Fig. 3 reflect the shape of $g(r_0)$ over the range of r_0 for which DFT band-structure calculations were available. Of course, the function $f(z)$ enters the plots when interpreted using Eq. (2), and is only available for coordination numbers $z=$ 12, 8, and 6; from Refs. 10 and 25

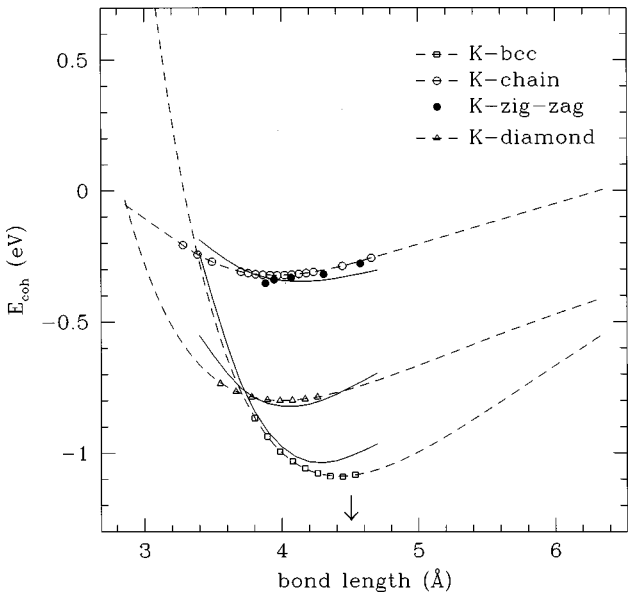

FIG. 4. Continuous line: plots of the cohesive energy $E_c(z,r_0)$ for K lattices corresponding to coordination numbers $z=$ 8, 4, and 2 from the quantum-chemical model in Eq. (2) as a function of the nearest-neighbor bond length. Dashed lines, squares, triangles, and open and closed circles correspond to the *ab initio* calculations of Fig. 2 for the same coordinations as before. The simple quantum-mechanical model is able to reproduce the main features and tendencies of the full calculation. In constructing the curves for $z=8$, 4, and 2, the quantity $f(z)$ in Eq. (1) was taken as $f(8)=4$, $f(4)=2.9$, and $f(2)=1.3$ (see text for details). The experimental bond length of K-bcc bulk (4.52 Å) (Ref. 30) is indicated by the vertical arrow.

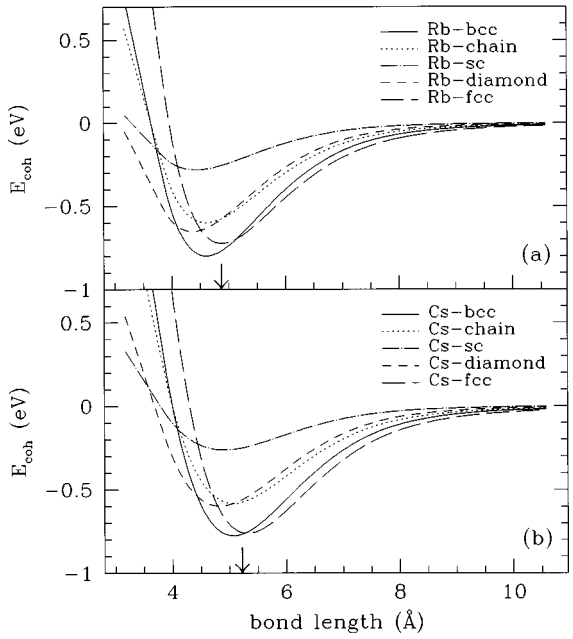

FIG. 5. Cohesive energy curves $E_c(z,r_0)$ for (a) Rb and (b) Cs atoms with long-range order in bcc, diamond, fcc, simple cubic, and linear chain structures (coordinations ranging from $z=12$ to $z=2$) as a function of the nearest-neighbor bond length. The experimental Rb (Cs) bulk bcc bond length of 4.83 Å (5.23 Å) is indicated by the vertical arrow. The results for Cs are relevant here in view of the interest in the bcc bulk metal and in highly expanded Cs chains with both short-range (Ref. 29) and long-range (Ref. 7) order.

the values of $f(z)$ are known to be equal to 4, 4, and 3, respectively. While presently we do not have an analytic form for $f(z)$, we know it is a slowly varying function of z as compared to the first term in Eq. (2). Below we shall provide estimates of $f(z)$ for $z=4$ and $z=2$ that match this behavior, but as March and co-workers[10] point out, for lattices other than bipartite lattices, first-principles calculations of $f(z)$ beyond perturbation theory present substantial difficulties. Turning to the lowest curve in Fig. 3, we have plotted the *ab initio* linear chain data as well as (supplemented) some ''zig-zag'' chain data (filled circles in Fig. 3). Obviously, there is some ''residual'' dependence of the cohesive energy $E_c(z,r_0)$ on second-neighbor interactions, which is ignored in writing the approximate form in Eq. (2). Indeed, below a certain value of r_0, there is some ''scatter'' for lattices with the same coordination z (2 for these chains).

From the work of Poshusta and Klein[26] on hydrogen, and Malrieu and co-workers on Na (Ref. 25) based on a cluster-expanded *ab initio* Heisenberg spin Hamiltonian, one can interpret $g(r_0)$ in Eq. (2) as reflecting the ''exchange'' part of the dimer potential energy curve that is half the difference between singlet and triplet potential-energy curves for the free space dimer. Theoretical values of these $^1\Sigma_g$ and $^3\Sigma_u$ potential energies are available from the work of Krauss and Stevens[27] and from their Table I(A) we have constructed the ''exchange'' $g(r_0)$ in Eq. (1) (see also Zemke and co-workers[28] for a complete experimental analysis of the K-dimer singlet and triplet states). This ''exchange'' part compares well with the ''extracted'' forms predicted from the difference of cohesive energy calculations in Fig. 3. To fit these cohesive energy differences grossly using the theoretical values for $g(r_0)$, we need to choose $f(z=4)\sim 2.9$ and $f(z=2)\sim 1.3$. This extends the available set of values of the smooth function $f(z)$ to the range $2\leqslant z\leqslant 12$ for the heavier alkalis. To complete the description of the quantum-chemical model of Eq. (1) we can relate[10] the function $R(r_0)$, ''eliminated'' in the plots of the band-structure cohesive energy differences in Fig. 1, to the $^3\Sigma_u$ potential-energy curve of the dimer given also in Ref. 27.

In Fig. 4 we present the results for the cohesive energy of the present quantum-chemical model for different extended K structures (bcc, diamond, and chains) compared with the *ab initio* calculations from Fig. 2. We have used $g(r_0)$ and $R(r_0)$ obtained from the singlet and triplet potential-energy curves of the free space K_2 dimer, to calculate the quantum-chemical approximation to $E_c(z,r_0)$ in Eq. (2). While, of course, the band calculations are expected to be fully quantitative, we observe that the main features such as bond length, bulk modulus, and cohesive energy are successfully reproduced within a few percent error by the quantum-chemical formula of Eq. (2). We have thought it of interest to add data for Rb and Cs from Eq. (2), using again the work of Krauss and Stevens for the corresponding free space dimers.[27] In both cases various coordinations (between 2 to 12) are studied by using the ''universal'' $f(z)$ (Ref. 10) function for the heavier alkalis previously obtained for K. In Fig. 5 we show the results for Rb and Cs. For the ground-state bcc structure of both metals the quantum-chemical bond length is smaller than the experimental one by a few percent. The curves for Cs are of interest in relation to the neutron-

scattering experiments of Hensel and co-workers[29] on this metallic fluid along the liquid-vapor coexistence curve. Also the work of Whitman *et al.*[7] in which Cs chains (zig-zag) are found when Cs is adsorbed on GaAs and InSb semiconducting substrates is relevant here (see previous section on low-coordination phases).

V. CONCLUSIONS

In summary, local coordination seems to exhibit similar trends with density for all the heavier alkali metals. In the liquid state the bond length remains remarkably constant when the density is varied from the normal melting point to twice the critical density. However when grown on semiconductor substrates, the nearest-neighbor distances are imposed by these substrates. Nevertheless, at low coverage the Cs atoms take up zig-zag chain configurations with low-coordination numbers as found in the expanded liquid phase. The present calculations on K atoms support the zig-zag chains as possible structures in the low-coordination regimes both in the liquid phase and on semiconductor surfaces. Similar results are expected to hold for the other alkali metals (Rb and Cs) in agreement with available experiments. Furthermore, in Fig. 3 we have presented DFT band-theory data of three K lattices: bcc, diamond, and chains in a form in which contact can be established with the quantum-chemical form of Eq. (2). $g(r_0)$ is the ''exchange'' part of the dimer problem[10,28] and the shapes of the band-theory cohesive energy curves reflect rather directly the dimer form of $g(r_0)$. This has encouraged us to plot the cohesive energy curves from Eq. (2), using $R(r_0)$ from the $^3\Sigma_u$ triplet potential-energy curve of the K dimer.[27] The main features of the band-theory results are thereby obtained, very simply, using values for $f(z)$ in Eq. (2) extracted from *ab initio* calculations. We have extended these results by using the dimer curves to construct the cohesive energy curves for long-range ordered arrays of Rb and Cs atoms. The representation of the cohesive energy in Eq. (2) by coordination-dependent functions naturally led to a coordination-dependent pair potential determined from properties of the dimer.[10] The relevance of Eq. (2) for other systems than the alkalis, as hydrogen lattices, is presently under study.

ACKNOWLEDGMENTS

A.R. acknowledges financial support from DGES (Grant Nos. PB95-0720 and PB95-0202) and Junta de Castilla y León (Grant No. VA25/95). One of us (N.H.M.) performed most of his contribution to this study during a visit to the University of Valladolid in 1996. He wishes to thank J. A. Alonso and his colleagues for the very stimulating environment they provided and for generous help and G. R. Freeman for numerous invaluable discussions on the nature of chemical bonding in highly expanded Rb and Cs. N.H.M. also acknowledges partial financial support from the Leverhulme Trust, UK, for work involving density-functional theory.

[1] R. Winter, F. Hensel, T. Bodensteiner, and W. Gläser, Ber. Bunsenges. Phys. Chem. **91**, 1327 (1987); J. Phys. Chem. **92**, 7171 (1988).

[2] R. Winter and F. Hensel, Phys. Chem. Liquids **20**, 1 (1989).

[3] N. H. March, Phys. Chem. Liquids **20**, 241 (1989); J. Math. Chem. **4**, 271 (1990).

[4] J. A. Ascough and N. H. March, Phys. Chem. Liquids **21**, 251 (1990).

[5] M. D. Johnson and N. H. March, Phys. Lett. **3**, 313 (1963).

[6] T. Arai and I. Yokoyama, Phys. Chem. Liquids **26**, 143 (1993).

[7] L. J. Whitman, J. A. Stroscio, R. A. Dragoset, and R. J. Celotta, Phys. Rev. Lett. **66**, 1338 (1991).

[8] See also P. N. First, R. A. Dragoset, J. A. Stroscio, R. J. Celotta, and R. M. Feenstra, J. Vac. Sci. Technol. A **7**, 2868 (1989).

[9] G. R. Freeman and N. H. March, J. Phys. Chem. **98**, 9486 (1994).

[10] N. H. March, M. P. Tosi, and D. J. Klein, Phys. Rev. B **52,** 9115 (1995). Equation (2) of this work shows the ''universality'' behavior of the function $f(z)$. However, for other than bipartite lattices one must assume that frustration can be subsumed, at least approximately, into the function $f(z)$.

[11] M. L. Cohen, Solid State Commun. **92**, 45 (1994); Phys. Scr. **1**, 5 (1982); J. Ihm, A. Zunger, and M. L. Cohen, J. Phys. C **12**, 4409 (1979).

[12] W. E. Pickett, Comput. Phys. Rep. **9**, 115 (1989); M. C. Payne, M. P. Teter, D. C. Allan, T. A. Arias, and J. D. Joannopoulos, Rev. Mod. Phys. **64**, 1045 (1992).

[13] D. M. Ceperly and B. J. Alder, Phys. Rev. Lett. **45**, 566 (1980); J. P. Perdew and A. Zunger, Phys. Rev. B **23**, 5048 (1981).

[14] N. Troullier and J. L. Martins, Solid State Commun. **74**, 613 (1990); Phys. Rev. B **43**, 1993 (1991).

[15] S. G. Louie, S. Froyen, and M. L. Cohen, Phys. Rev. B **26**, 1738 (1982).

[16] In the present calculations by changing the density (expanded nearest-neighbor distance) of the condensed phase we take a partial account of substrate-adsorbate interaction. In this simplified picture the role of the substrate is to fix the bond length of the adsorbed metal.

[17] K. P. Huber and G. Herzberg, *Constants of Diatomic Molecules* (Van Nostrand, Princeton, 1977).

[18] The possible formation of general three-dimensional ''walks'' as compared to the in-plane zig-zag chains studied here is very difficult to address from the present *ab initio* calculations based on periodic boundary conditions. However, the computed Born-Oppenheimer surface for the zig-zag chain is rather flat, indicating a potential three-dimensional ''floppy'' behavior for the K chain. This suggests that three-dimensional walks have a very small effect on the total energy and they can be neglected for the present study.

[19] A. Ferraz, N. H. March, and F. Flores, J. Phys. Chem. Solids **45**, 627 (1984).

[20] M. C. Gutzwiller, Phys. Rev. Lett. **10**, 159 (1963); Phys. Rev. **134**, A923 (1964); **137**, A1726 (1965).

[21] C. A. Coulson and I. Fischer, Philos. Mag. **40**, 386 (1949).

[22] See also G. Senatore and N. H. March, Rev. Mod. Phys. **66**, 445 (1994).

[23] The fundamental support for the factorization *ansatz* in the second term of Eq. (2) rests on expanding a Heisemberg Hamiltonian in a sum of irreducible cluster interaction operators. For a

cluster length ($N=2$) the Hamiltonian parameters are completely determined by the singlet and triplet states of the dimer (for more details see Refs. 26 and 25).

[24] M. W. Finnis and J. E. Sinclair, Philos. Mag. A **50**, 45 (1984).

[25] J. P. Malrieu, D. Maynau, and J. P. Daudey, Phys. Rev. B **30**, 1817 (1984).

[26] R. D. Poshusta and D. J. Klein, Phys. Rev. Lett. **48**, 1555 (1982).

[27] M. Krauss and W. J. Stevens, J. Chem. Phys. **93**, 4236 (1990).

[28] W. T. Zemke, C. C. Tsai, and W. C. Stwalley, J. Chem. Phys. **101**, 10 382 (1994).

[29] See, for example, R. Winter, W. C. Pilgrim, and F. Hensel, J. Phys.: Condens. Matter **6**, A245 (1994).

[30] C. Kittel, *Introduction to Solid State Physics*, 6th ed. (Wiley, New York, 1986).